EXPERIMENTAL STUDY ON NON-EQUILIBRIUM TURBULENT BOUNDARY LAYER WITH SEPARATION, REATTACHMENT, AND REDEVELOPMENT

Simon Song
Department of Mechanical Engineering, Stanford University
Stanford, CA 94305-3030, USA
simons@stanford.edu

John K. Eaton
Department of Mechanical Engineering, Stanford University
Stanford, CA 94305-3030, USA
eaton@vonkarman.stanford.edu

ABSTRACT
A non-equilibrium boundary layer with separation, reattachment, and redevelopment is measured using a high resolution LDA for a large range of Reynolds number. The mean separation and reattachment positions are not a function of Reynolds number. The recovering boundary layer develops a stress equilibrium layer. Independent skin friction measurements confirmed that the law of the wall is valid in the redevelopment region. At separation, each of the three measured Reynolds stress components scales differently. At reattachment, none of the Reynolds stresses collapse for the given Reynolds number range. In the redevelopment region, all Reynolds stress components are scaled like a flat plate boundary layer within the stress equilibrium layer.

INTRODUCTION
DeGraaff and Eaton (2000) showed that non-dimensional ratios of Reynolds stresses in the flat plate boundary layer are weak functions of the Reynolds number. They found that the streamwise Reynolds normal stress scales on the product of freestream velocity and friction velocity over a range of momentum thickness Reynolds number (Re_θ) from 1430 to 31000. This is also supported by Metzger *et al.* (2001) including data up to $Re_\theta = 5\times10^6$. This fact poses difficulties in applying many turbulence models to high Reynolds number flows. Variations in turbulence modeling parameters with Reynolds number are likely to be stronger in non-equilibrium boundary layers which have additional length scales beyond the inner and outer scales that characterize flat-plate flows.

DeGraaff and Eaton (1999) suggested that a stress equilibrium layer develops when a turbulent boundary layer recovers from perturbation. The stress equilibrium layer is in equilibrium with the local wall shear stress and grows out through the non-equilibrium boundary layer. Song *et al.* (2000) examined a non-equilibrium boundary layer downstream of a small separation bubble. They found that a stress equilibrium layer develops quickly after reattachment, but grows slowly in the downstream redevelopment region.

The present study addresses the characteristics of a non-equilibrium turbulent boundary layer with separation, reattachment, and redevelopment over a range of reference momentum thickness Reynolds numbers from 1100 to 20300. We discuss the Reynolds number effects on separation and reattachment. The validity of using log-law fitting to obtain skin friction data in a non-equilibrium boundary layer is also discussed. Finally, we place particular emphasis on Reynolds number scaling of the Reynolds stresses in the non-equilibrium boundary layer.

EXPERIMENTAL APPARATUS
The experiments were performed using a high Reynolds number wind tunnel (DeGraaff and Eaton, 2000). It is a lab-scale, closed-loop wind tunnel mounted entirely inside a large pressure vessel. By increasing the vessel pressure up to 8 atm and changing the tunnel speed by a factor of three, we can achieve a Reynolds number ratio of 24:1 at a single measurement position without changing any other parameters. A custom-built, two-component, high-resolution Laser Doppler Anemometer (LDA) with a measurement volume 35 μm in diameter by 60 μm in length provided sufficient resolution to resolve all turbulence scales over the full range of Reynolds numbers. Uncertainties for U, $\overline{u'u'}$, $\overline{v'v'}$, and $\overline{u'v'}$ were estimated as ± 1.5 %, ± 4 %, ± 8 %, and ± 10 % of their local value in the center of profiles, respectively (DeGraaff and Eaton, 2001).

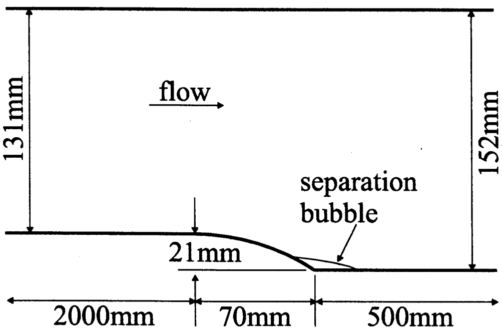

Figure 1 : Flow geometry.

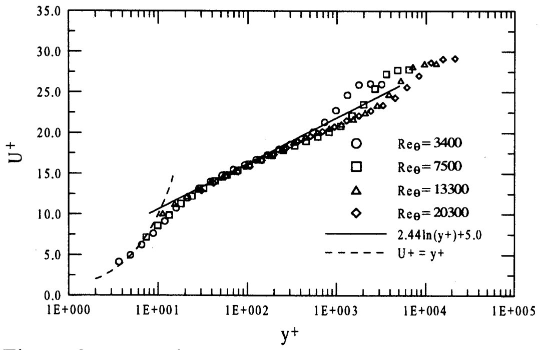

Figure 2 : Law of the wall at x' = 7.00.

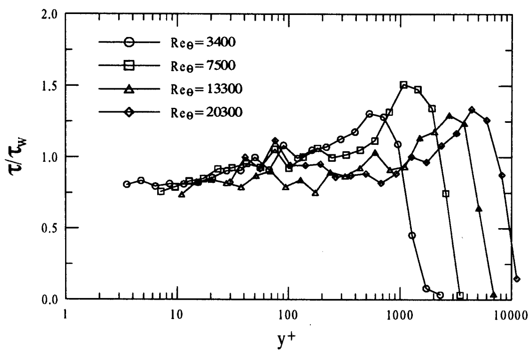

Figure 3 : Total shear stress at x' = 7.00.

The flow geometry is shown in Fig. 1. A two-dimensional turbulent boundary layer develops on an upstream flat plate. The mean flow separates about 2/3 of the way along the ramp making a small separation bubble over the trailing edge of the ramp. The flow reattaches on a downstream flat plate where the boundary layer redevelops (Song *et al.*, 2000).

Skin friction was measured by an oil-fringe imaging technique (Monson *et al.*, 1993) in the redevelopment region for all Reynolds numbers except for $Re_{\theta,ref}$ = 1100. To reduce uncertainty, simultaneous oil-fringe measurements were performed in a region with known skin friction and at a point of interest. Dow Corning 200 fluids with the viscosity of 50 cs, 100 cs, 200 cs, and 350 cs were used for $Re_{\theta,ref}$ = 3400, 7500, 13300, and 20300, respectively. A Kodak high-resolution digital camera (Model DC290) was used for imaging oil-fringes. A green monochrome light source was used. The imaging surface was a 0.13 mm thick, green acetate, back-side-painted flat black. The resulting images had at least 4~6 clear fringes. This oil-fringe method was found to be very accurate. The method was verified by comparing its results with mean velocity gradient measurements in the sublayer at $Re_{\theta,ref}$ = 3400 at both an upstream reference location and the most downstream location in the non-equilibrium boundary layer. The oil-fringe method and the velocity gradient measurements agree within 10 %.

RESULTS AND DISCUSSION

Mean properties

The coordinate system is such that x' indicates streamwise locations normalized by the ramp length. The beginning of the ramp is set to x' = 0.00 and the ramp trailing edge is set to x' = 1.00. The reference station corresponds to x' = -2.00 where a flat plate boundary layer develops. The vertical height, y, is maintained normal to the flat plate throughout the entire flow geometry.

Detailed LDA measurements are complete for five $Re_{\theta,ref}$'s (1100, 3400, 7500, 13300, and 20300). Song *et al.* (2000) reported flow characteristics at a single Reynolds number ($Re_{\theta,ref}$ = 3500) for the same geometry as the present case. These flow characteristics are identical to $Re_{\theta,ref}$ = 3400 of the

$Re_{\theta,ref}$	$Re_{\theta,x'=7}$	Log-law fitting			Oil-fringe method		
		$C_f \times 10^3$	τ_w [Pa]	U_τ [m/s]	$C_f \times 10^3$	τ_w [Pa]	U_τ [m/s]
3400	5500	2.92	0.58	0.70	2.94	0.59	0.68
7500	13500	2.43	0.58	0.35	2.59	0.62	0.35
13300	24600	2.35	2.12	0.62	2.46	2.22	0.62
20300	39100	2.19	3.40	0.61	2.29	3.55	0.61

Table 1 : Comparison of skin friction data at x' = 7.00.

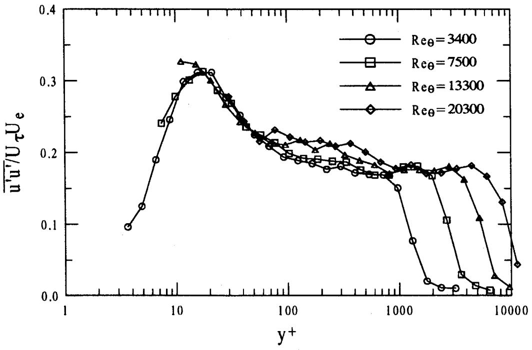

Figure 10 : Streamwise Reynolds normal stress at x' = 7.00.

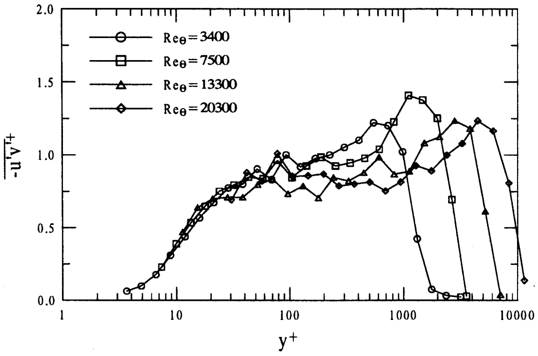

Figure 11 : Reynolds shear stress at x' = 7.00.

friction used to calculate U_τ in Fig. 2 comes from the oil-fringe measurements, not from a log-law fit.

The validity of using the log-law fitting in order to obtain skin friction information in a non-equilibrium boundary layer is of interest. Table 1 compares skin friction data obtained from the log-law fitting and from the oil-fringe method at x' = 7.00. The two methods are in good agreement within 5% in skin friction coefficient.

The near-wall flow is in equilibrium with the local wall shear stress at x' = 7.00. Fig. 3 shows the total shear stress profiles at x' = 7.00. The constant shear stress region extends to $y^+ = 60$. This constant shear stress region is the stress equilibrium layer.

Because it is dominated by large, essentially inviscid eddies, the mean flow recovery is relatively independent of Reynolds number. The ratio of skin friction coefficient at a position (x' = 4.00 or 7.00) to at a reference position (x' = -2.00) is independent of Reynolds number over the present Reynolds number range. The ratio is approximately 0.70 at x' = 4.00 and 0.71 at x' = 7.00.

Reynolds number scaling

The upstream Reynolds stresses at x' = -2.00 show the same Reynolds number scaling seen by DeGraaff and Eaton (2000) in the flat plate turbulent boundary layer. The streamwise Reynolds normal stress was scaled by a so-called mixed scaling, $U_\tau U_e$. The wall normal Reynolds stress and Reynolds shear stress were scaled by the classical inner scaling, U_τ^2.

The mixed scaling, however, does not collapse the streamwise Reynolds normal stress in a favorable pressure gradient region. At x' = 0.00 where a mild favorable pressure gradient is caused by the convex curvature of the ramp, the streamwise Reynolds normal stress does not scale on either the mixed scaling or the classical inner scaling. The peak intensity increases with increasing Reynolds number in both scalings.

In the strong adverse pressure gradient region where the flow separates (x' = 0.73~0.76), the various Reynolds stress components seem to scale differently. The streamwise normal stress does not collapse on any known scales (Fig. 4), the shear stress collapses on the outer scale (Fig. 5), and the wall normal stress collapses on the upstream inner scale (Fig. 6). The peaks in the Reynolds stress components indicate the large eddies generated by the Kelvin-Helmholtz instability. Note that the peaks of the Reynolds stresses align closely with the inflection point heights in the mean profiles. This inflection point height collapses the positions of the large eddies not only in this adverse pressure gradient region but also in the redevelopment region when the large eddies are carried downstream. The inflection point height is clearly an important length scale in the current flow.

At reattachment (x' = 1.36~1.40), none of the known scales collapse Reynolds stresses. Eaton and Johnston (1981) showed that Reynolds stress started to decay approximately one step height upstream of reattachment for the backward-facing step flows. Song *et al.* (2000) reported that the peaks in Reynolds stress components at reattachment are either equal to or slightly higher than at the ramp trailing edge (x' = 1.00). Although Reynolds stress profiles at the ramp trailing edge are not presented here, the reattachment profiles in Fig. 7~9 show that the peaks of all three Reynolds stresses have increased through the separated region. In addition, the growth rate of the peak throughout the separated region is also a function of Reynolds number. The peaks in all three Reynolds stress components increase with increasing Reynolds number. As a result, the growth of the peaks throughout the separated region is more evident for the higher Reynolds numbers.

Downstream of reattachment, the Reynolds stresses do not recover to their canonical flat plate characteristics as rapidly as the mean quantities due to the large eddies carried from the separation region. The present results confirm that a stress equilibrium layer grows downstream of reattachment. Fig. 10 and 11 show the streamwise Reynolds normal stress and Reynolds shear stress at the most downstream location (x' = 7.00). The

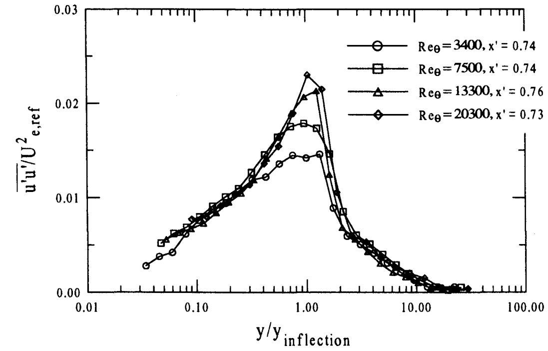

Figure 4 : Streamwise Reynolds normal stress at separation.

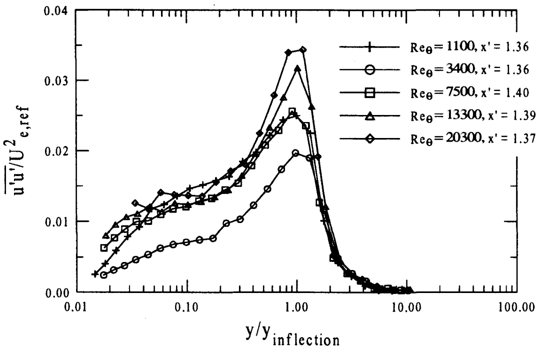

Figure 7 : Streamwise Reynolds normal stress at reattachment.

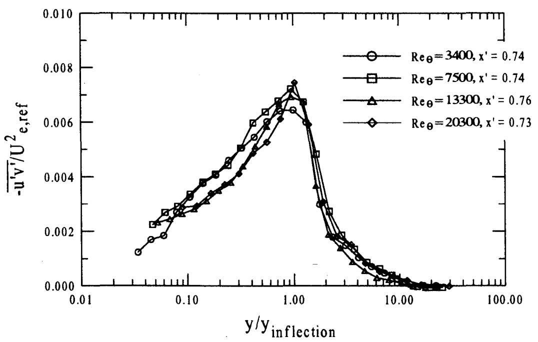

Figure 5 : Reynolds shear stress at separation.

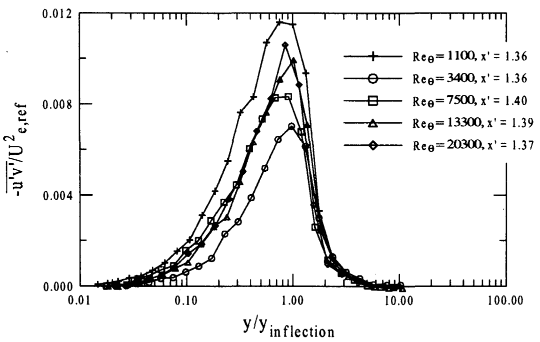

Figure 8 : Reynolds shear stress at reattachment.

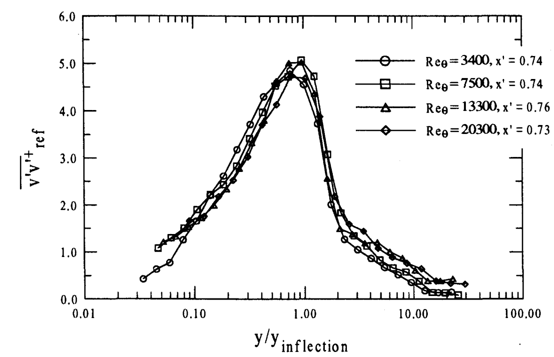

Figure 6 : Wall-normal Reynolds normal stress at separation.

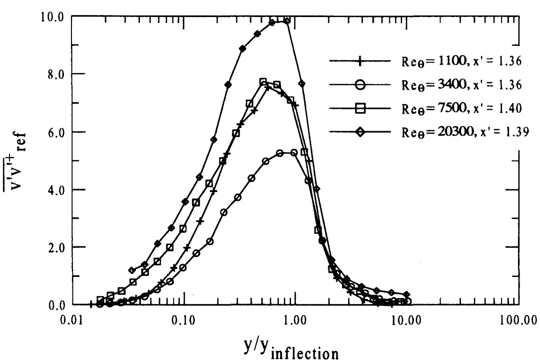

Figure 9 : Wall-normal Reynolds normal stress at reattachment.

present experiments. The mean flow development is insensitive to Reynolds number except for the lowest Reynolds number case which separates about 25 mm earlier than the other cases. All other cases give a separation bubble length of approximately 44 mm with separation at x' = 0.73~0.76 and reattachment at x' = 1.36~1.40. However, Song and Eaton (2001) showed that the separation bubble length is increased by approximately 70 % when wall roughness is introduced for the same flow geometry as the present case. This fact implies that changes presumably seen in a separated region at high Reynolds numbers might be caused by the hydrodynamic wall-roughness effects rather than Reynolds number effects.

The mean flow recovery appears to be very rapid at all Reynolds numbers. At the most downstream location (x' = 7.00), the mean velocity profile appears completely recovered when normalized by the freestream velocity and the boundary layer thickness. The logarithmic plot (Fig. 2) also shows that the boundary layer has almost recovered to canonical behavior. The dip below the standard log-law value is a typical characteristic of the non-equilibrium boundary layer. Note that the skin stresses in the inner layer collapse up to $y^+ = 60$ where the stress equilibrium layer extends. Although the wall normal Reynolds stress component is not shown, it also collapses in the inner coordinate system up to $y^+ = 60$. This implies that simple single point models can be applied adjacent to the wall in the redevelopment region of the turbulent boundary layer. The large eddies are still evident in the outer boundary layer. This is one of typical characteristics of a non-equilibrium boundary layer. Although it is not shown here, the Reynolds stress peaks in the outer layer collapse when the vertical height is normalized by the inflection point height in the separated region.

CONCLUSION

A non-equilibrium boundary layer with separation, reattachment, and redevelopment was investigated for a range of momentum thickness Reynolds number from 1100 to 20300. The mean separation and reattachment positions are not a function of Reynolds number except for the lowest Reynolds number case. Independent skin friction measurements show that the law of the wall is still valid in the redevelopment region. A stress equilibrium layer develops downstream of reattachment and it extends to $y^+ = 60$ at the most downstream location. The skin friction ratio of a non-equilibrium boundary layer to a flat plate boundary layer is constant over the full range of Reynolds number.

The mixed scaling collapses the streamwise Reynolds normal stress in a flat plate boundary layer. However, the mixed scaling does not work in a favorable pressure gradient. Near separation, none of the known scalings collapse the streamwise Reynolds normal stress, but the reference outer scaling and the reference inner scaling collapse the Reynolds shear stress and the wall-normal Reynolds stress, respectively. At reattachment, none of Reynolds stress components collapse in a known scaling. The Reynolds stress peaks grow through the separated region and the growth rate is a function of Reynolds number. In the redevelopment region, the streamwise Reynolds normal stress scales on the local mixed scaling within the stress equilibrium layer. The Reynolds shear stress and the wall normal stress scale on the local inner scales.

References

DeGraaff, D. B., and Eaton, J. K., 1999, "Reynolds Number Scaling of the Turbulent Boundary Layer on a Flat Plate and on Swept and Unswept Bumps", Report No. TSD-118, Stanford Univ., Stanford, CA.

DeGraaff, D. B., and Eaton, J. K., 2000, "Reynolds Number Scaling of the Flat Plate Turbulent Boundary Layer", J. Fluid Mech., Vol. 422, pp. 319-346.

Eaton, J. K., and Johnston, J. P., 1981, "A Review of Research on Subsonic Turbulent Flow Reattachment", *AIAA J.*, Vol. 19, No. 9, pp. 1093-1100.

Metzger, M. M., Klewicki, J. C., Bradshaw., K. L., and Sadr, R., 2001, "Scaling the Near-Wall Axial Turbulent Stress in the Zero Pressure Gradient Boundary Layer", *Phys. Fluids*, submitted.

Monson, D. J., Mateer, G. G., Menter, F. R., 1993, "Boundary-Layer Transition and Global Skin Friction Measurement with an Oil-Fringe Imaging Technique", SAE Technical Paper Series 932550, Aerotech '93, Costa Mesa, CA, Sep. 27-30, 1993.

Song, S., DeGraaff, D. B., and Eaton, J. K., 2000, "Experimental Study of a Separating, Reattaching, and Redeveloping Flow over a Smoothly Contoured Ramp", *Inter. J. Heat and Fluid Flow*, Vol. 21, pp. 512-519.

Song, S., and Eaton, J. K., 2001, " The Effects of Wall Roughness on Turbulent Boundary Layers in Zero and Adverse Pressure Gradient", *Phys. Fluids*, submitted